IEICE TRANS. COMMUN., VOL.E103–B, NO.12 DECEMBER 2020

INVITED PAPER *Special Section on IoT Sensor Networks and Mobile Intelligence*

An Overview of Aerial Wireless Relay Networks for Emergency Communications during Large-Scale Disasters

Hiraku OKADA[†a)], ***Senior Member***

SUMMARY In emergency communication systems research, aerial wireless relay networks (AWRNs) using multicopter unmanned aerial vehicles (UAVs) have been proposed. The main issue of the AWRNs is how to minimize the delay time of packet transmissions since it is not easy to supply many multicopters to cover a wide area. In this paper, we review the flight schemes and their delay time for the AWRNs. Furthermore, the network has specific issues such as multicopters' drops due to their battery capacity depletion and inclination of moving multicopters. The inclination of multicopters affects the received power, and the communication range changes based on the inclination as well. Therefore, we clarify the effect of these issues on the delay time.

key words: *aerial wireless relay networks, multicopter UAV, delay time, flight schemes*

1. Introduction

The effect of the 2004 Mid Niigata Prefecture Earthquake serves the primary research question of this paper. The magnitude of the earthquake is M6.8, and the intensity on the Japanese seven-stage seismic scale is 7. In Yamakoshi village, as a lot of landslides destroyed lifelines, the village stood alone. The infrastructures of communication networks were damaged; the villagers could not cry for help from the outside of the village. It was challenging for the people inside and outside the village to collect information from the disaster-stricken areas. Consequently, therefore, we identify the need for emergency communication systems during large-scale disasters.

K. Mase et al. started the project, SKYMESH, to construct an ad hoc network in the sky for large-scale disaster recovery [1]–[3]. In SKYMESH, balloons float at 50–100 m above the ground, with wireless nodes suspended from the balloons. The wireless nodes communicate with each other via wireless transmissions and construct an ad hoc network in the sky. Due to the significant locations of the balloons, SKYMESH has advantages of good line-of-sight (LoS), long transmission distance, and low interference from wireless systems on the ground.

Nowadays, the technologies of unmanned aerial vehicles (UAVs) are rapidly developed and widely used in various fields. For example, in [4], a fixed-wing mini UAV is used for a wireless relay system to extend communication capability to the disaster-stricken area. Further, in our previous work, We proposed an aerial wireless relay network (AWRN) using multicopter UAVs to construct an ad hoc in the sky [5]–[7]. Unlike balloons, multicopters fly within a disaster-stricken area. Also, the reason to use multicopters is their mobility, which allows us to employ the technology of disruption-tolerant networking (DTN) [8]. Although the multicopters cannot be supplied enough to make the connections among them, moving the multicopters sustains the network.

The main issue of the AWRN is how to reduce the delay time of packet transmissions since it is not easy to supply many multicopters to cover a wide area. Unlike wireless communications, the delay time by multicopters' movement is significant. Thus, to minimize the delay time depends on how the multicopters move, which we call a flight scheme.

Thus, in this paper, we study the AWRN using multicopters and flight schemes to minimize the delay time. Although our research group has been investigating the flight schemes and their delay time [6], [7], [9], we review these studies and discuss the feasibility of the AWRN for emergency communication systems during large-scale disasters.

Then, the remainder of this paper is organized as follows: We compare the features of a balloon and multicopter in Sect. 2 and discuss the AWRN in Sect. 3. The network has particular issues we considered, which are discussed in Sects. 4 and 5. Finally, Sect. 6 presents the conclusions of this paper.

2. Balloon versus Multicopter

Table 1 compares the features of a balloon and multicopter. The balloon is tethered to a fixed point on the ground; therefore, it cannot move. The power can be supplied by either a battery in the wireless node or wire from the ground. The weight of the balloon is about 13 kg, and its size is about 8 m $\times$ 4 m [1]. The treatment of a balloon is not easy; however, it can float for a long duration until the balloon deflates.

Whereas, the multicopter flies with a battery. Compared with the balloon, the multicopter can move with high speed, the weight is light, and the size is smaller. The flight duration is short due to the battery limitation, but it is possible to supply power to the multicopter from the ground using wire. In this case, the flight duration becomes long, but mobility is lost.

Manuscript received February 27, 2020.
Manuscript revised April 7, 2020.
Manuscript publicized July 1, 2020.

[†]The author is with the Institute of Materials and Systems for Sustainability, Nagoya University, Nagoya-shi, 464-8603 Japan.
a) E-mail: hiraku@m.ieice.org

DOI: 10.1587/transcom.2020SEI0001

Table 1 Comparison between a balloon and multicopter.

	Balloon	Multicopter	
			
Power supply	Battery/wire	Battery	Wire
Weight	Heavy (about 13 kg)	Light (about 1 kg)	
Size	Large	Small	
Flight duration	Long (more than 10 h)	Short (20–40 min)	Long
Mobility	N/A	Max. 50 km/h	N/A

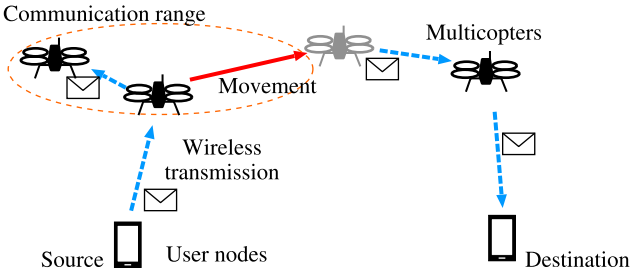

Fig. 1 An aerial wireless relay network.

3. An Aerial Wireless Relay Network

Figure 1 shows an aerial wireless relay network (AWRN) using the multicopters. The multicopters construct a wireless relay network in the sky, which serves as a backbone network. Also, each multicopter operates as an access point and accommodates user nodes on the ground. Then, a packet that is generated by a source node gets transmitted to a destination node through the AWRN. If a multicopter exists in the communication range of another multicopter, they can forward packets to each other. Otherwise, the packets get conveyed by the movement of the multicopters.

3.1 Flight Schemes

In the AWRN, flight schemes play an important role in minimizing the delay time. In addition, emergency communication systems are unexpectedly used when a large-scale disasters occurs. In this case, non-experts about networking might execute the operations of the emergency communication systems. Taking account of this situation, the flight schemes have to satisfy the following conditions:

- autonomous movement of multicopters without sophisticated settings,
- consideration of multicopters' drops due to depletion of the battery capacity, and
- ignorance of the information such as locations of the other multicopters before communications.

We use a random manner of multicopters' movement to satisfy the above conditions. When some multicopters drop due to the battery depletion, the other multicopters should compensate for them. If the multicopters move definitively, the flight scheme is sophisticated because it has to consider multicopters' drops, connections between multicopters, and coverage of user nodes on the ground.

In this section, we explain three flight schemes as follows.

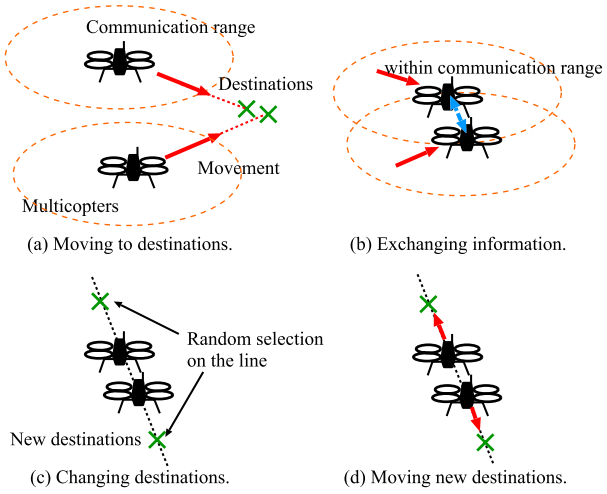

Fig. 2 The rebounding flight scheme.

(1) Random Waypoint

In general, the random waypoint (RWP) [10] is often used as an accidental movement. Here, each multicopter selects a point randomly in the disaster-stricken area and the position is regarded as a destination. The multicopter moves linearly to the destination, whereas the new destination got rearranged when the multicopter arrives at the current one.

Because of randomness of the RWP, there are sparse or dense areas of the distribution of multicopters within the stricken area. Furthermore, the distribution of multicopters is sparse in border areas of the disaster-stricken area due to border effects [11], [12]. In the dense area, communication ranges of the multicopters are overlapped, and the covering efficiency in the disaster-stricken area gets degraded.

(2) Rebounding

To avoid overlaps of communication ranges among multicopters, we proposed a rebounding flight scheme [6], [7]. Figure 2 shows the operation of the rebounding flight scheme. A multicopter does not have prior information about the positions of the other multicopters until information exchange between the multicopters. Like the RWP flight scheme, each multicopter moves to its destination. When a multicopter moves into the communication range of another multicopter, they exchange information about their locations. Using the current location information, they decide new destinations as follows: first, they draw the line through their positions. Next, each multicopter selects a new destination randomly between its location and the boundary of the disaster-stricken area opposite from the other multi-

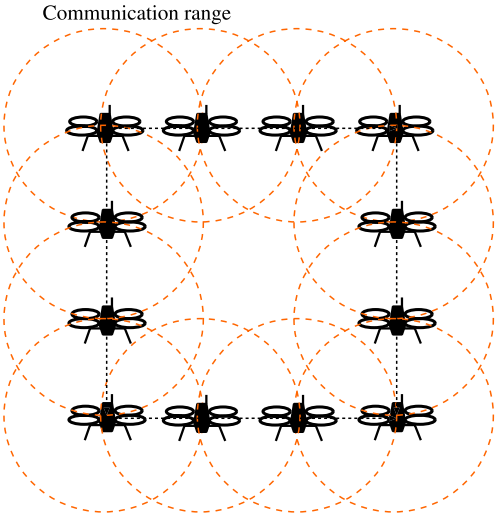

Fig. 3 A common flight path.

copter on the line. Finally, these multicopters move linearly to the new destinations.

By selecting the new destinations in the opposite directions, the multicopters move reboundingly. The rebounding movement can mitigate the overlap of their communication ranges.

(3) Common Flight Path

The common flight path (CFP) was proposed for the efficient forwarding of packets in [6], [7]. Here, some multicopters move on a predefined path and maintain connections between the neighboring multicopters. Figure 3 shows an example of the CFP, which is constructed as a square. The multicopters on the path fly within the communication range to each other to establish the connected network. Therefore, the multicopters on the CFP forward packets via wireless transmissions, and the delay time get minimized if the CFP is used effectively for the packet transmissions.

The multicopters on the CFP can move while keeping the network connectivity. Whereas, if the multicopters stay, a wired power supply can be used. The multicopters not belonging to the CFP obey the RWP or rebounding flight schemes.

3.2 Delay Time Evaluation

In this section, we evaluate the delay time of RWP, rebounding, and CFP flight schemes.

3.2.1 Simulation Conditions

When the CFP is introduced, some multicopters fly on the CFP, whereas others move according to the RWP or rebounding flight scheme. Here, we ignore the buffer size of the multicopters and use the epidemic routing protocol as the DTN. The delay time of wireless transmissions is ignored, as this delay is much shorter than that of packets carried by the multicopters. A network simulator is not used,

Table 2 Simulation settings.

Simulation area	4000 m × 4000 m
Position of source node	(500, 500)
Position of destination node	(3500, 3500)
Size of CFP	2000 m × 2000 m (16 multicopters)
Moving speed	10 m/s
Communication range	500 m

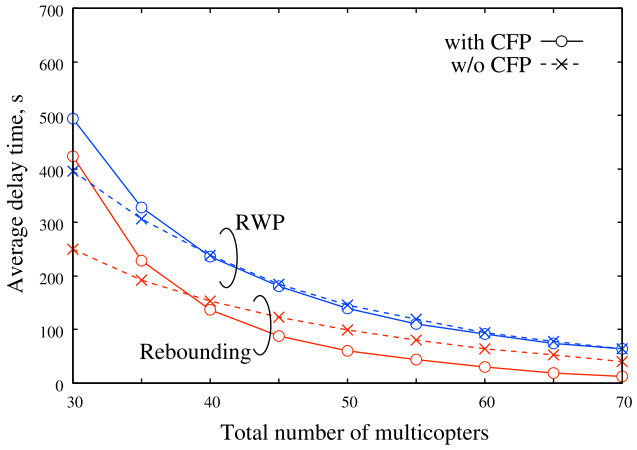

Fig. 4 Average delay time of RWP and rebounding flight schemes with and without CFP.

and the simulation is programmed by the C language.

Table 2 shows the simulation settings. The simulation area, which corresponds to the disaster-stricken area, is 4000 m × 4000 m. The positions of the source and destination nodes are (500, 500) and (3500, 3500), respectively. The shape of the CFP is rectangle, and its size is 2000 m × 2000 m. The CFP is located at the center of the simulation area. The moving speed of a multicopter is 10 m/s. Since the LoS can be kept among multicopters, the communication range becomes long, which we set to 500 m.

3.2.2 Numerical Examples

Figure 4 shows the average delay time of four different cases, i.e., RWP and rebounding flight schemes with and without CFP, where the total number of multicopters indicates the quantity of multicopters that move according to RWP or rebounding flight schemes, and at the same time stays on the CFP. From the figure, we found that the rebounding flight scheme minimizes the average delay time since the overlap of communication ranges of multicopters can be minimized. For the case of the rebounding flight scheme, the CFP is effective in reducing the average delay time when the total number of multicopters is greater than 40. Whereas, when the total number of multicopters is less than 40, the limited number of multicopters that obey the rebounding flight scheme causes an increase in the average delay time. For the RWP flight scheme, the improvement by the CFP is hard to come by.

Next, we discuss the effect of the rebounding flight

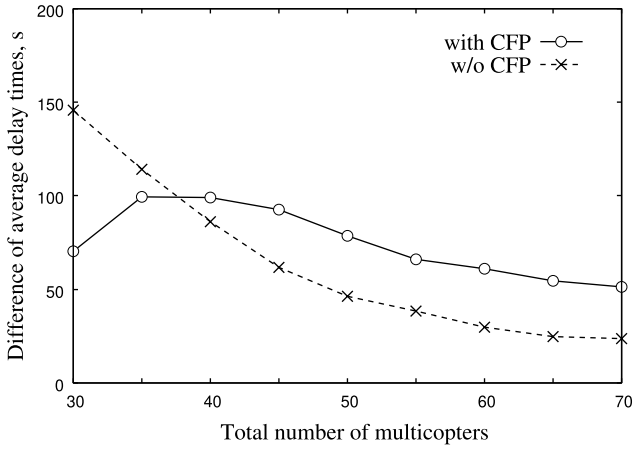

Fig. 5 The difference of the average delay times between RWP and rebounding flight schemes.

scheme. Figure 5 shows the difference in the average delay times between the RWP and the rebounding flight schemes. For the case without the CFP, the difference becomes insignificant as the total number of the multicopters becomes large. A good number of multicopters makes small the difference between them. For the case of using the CFP, the difference is insignificant when the total number of multicopters is 30. The multicopters that move according to the rebounding flight scheme is only 14. Then, the sparse of the moving multicopters degrades the effect of rebounding.

4. Consideration of Battery Depletion

Since the battery is limited, a multicopter has to drop and change its battery when the battery capacity gets depleted, which causes the degradation of the delay time. In this section, we investigate the effects of considering the multicopters' drops due to their battery depletion.

4.1 Model of Multicopters' Drops

To consider the multicopters' drops, we introduce flight and drop duration. Each multicopter flies for the flight duration, which is decided based on the battery capacity. When the flight duration expires, the multicopter drops out of the AWRN and stops flying during the drop duration to exchange its battery. In this period, the multicopter cannot send and receive packets. After the drop duration, the multicopter flies again and joins the network.

In this paper, we consider three timings to begin the drop duration: random, ordering, and synchronous schedules.

(1) Random Timing

Each multicopter drops at randomly independent timing. Hence, the multicopters need not arrange their drop timings for each other. In this case, the number of on-flying multicopters changes from time to time, and the delay time might fluctuate.

Table 3 Simulation settings for the evaluation considering multicopters' drops.

Simulation area	4000 m × 4000 m
Position of source node	(500, 500)
Position of destination node	(3500, 3500)
Size of CFP	2000 m × 2000 m (16 multicopters)
Moving speed	10 m/s
Communication range	500 m
Flight duration	20 min
Drop duration	10 min

(2) Ordering Timing

The drop timing of each multicopter occurs at a uniform interval; therefore, the number of flying multicopters is constant. The interval gets decided by dividing the sum of the flight and the drop duration by the total number of the multicopters. In this case, the drop timings have to be arranged among the multicopters to mitigate the fluctuation of the delay time.

(3) Synchronous Timing

All multicopters drop at the same timing. Here, all multicopters fly during the flight duration, or any multicopters do not operate during the drop duration. The delay time during the flight duration gets reduced.

4.2 Delay Time Evaluation Considering Multicopters' Drops

Here, we evaluate the delay time based on multicopters' drops. Table 3 shows the simulation settings. The flight and drop durations are 20 and 10 min, respectively. We use the simplified model in which the battery is exchanged on the ground at the same horizontal position when the battery capacity gets depleted. In actuality, the multicopters move to a recharging station before the battery depletion. The effect of the movement was evaluated in [7].

Figure 6 shows the average delay time of the RWP without the CFP, the rebounding without the CFP, and the rebounding with the CFP by using the random drop timing. The average delay time of the RWP with the CFP gets omitted since the improvement by the CFP cannot be obtained for the RWP. From this figure, we confirm that the consideration of multicopters' drops causes the increase of the average delay time. To clarify the rise due to multicopters' drops, we depict the increasing rate of the required total number of multicopters in Fig. 7, where the increasing rate is calculated by (the number of multicopters considering the drops required to achieve the target average delay time)/(that without the consideration of drops). For the case of the RWP flight scheme, the consideration of multicopters' drops causes the reduction of multicopters only. Therefore, the increasing rate is constant for the target average delay time. For the case of the rebounding without the CFP, the increasing rate becomes insignificant for the short average delay time. It is because the rebounding flight scheme can

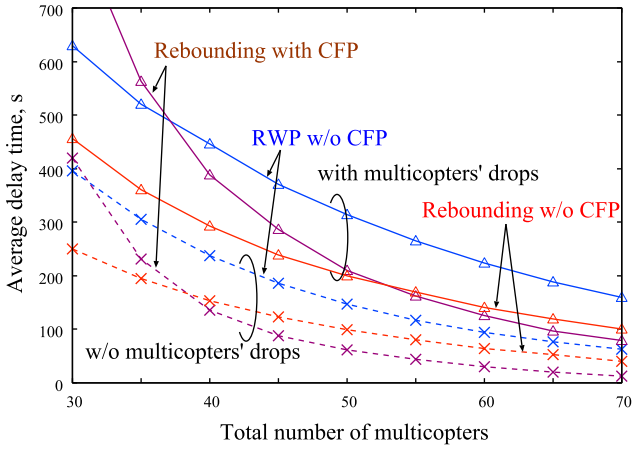

Fig. 6 Average delay time considering multicopters' drops.

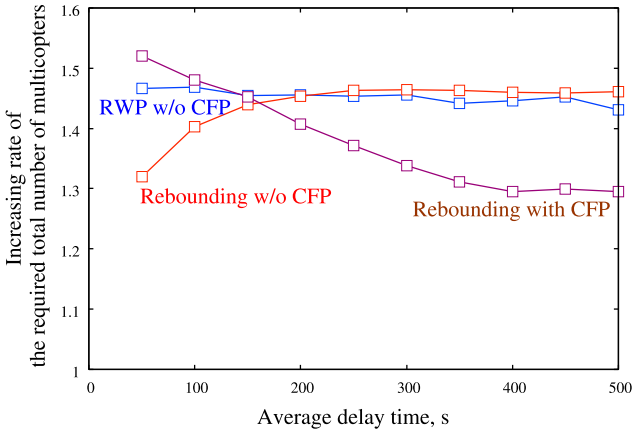

Fig. 7 Increasing rate of the total number of multicopters required to achieve the average delay time.

compensate for the drops of multicopters by rebounding. For the case of the rebounding with the CFP, the increasing rate is significant for the short average delay time, whereas it is insignificant for the long average delay time. Therefore, the CFP can mitigate the effects of multicopters' drops when the total number of multicopters is large.

To evaluate the difference among drop timings, Fig. 8 shows the average delay time of each drop timings for the rebounding flight scheme. We are to find a significant difference in the average delay time between the random and the ordering timings. Therefore, we do not have to arrange drop timings to keep the number of on-flying multicopters constant. When the CFP is not used, the average delay time of the random schedule is shorter than that of the synchronous timing. However, the synchronous timing achieves the shortest average delay time using the CFP. Then, if some multicopters on the CFP drops, the connectivity of the CFP cannot be kept. Therefore, we should arrange the drop timings of the multicopters on the CFP to maintain the connectivity.

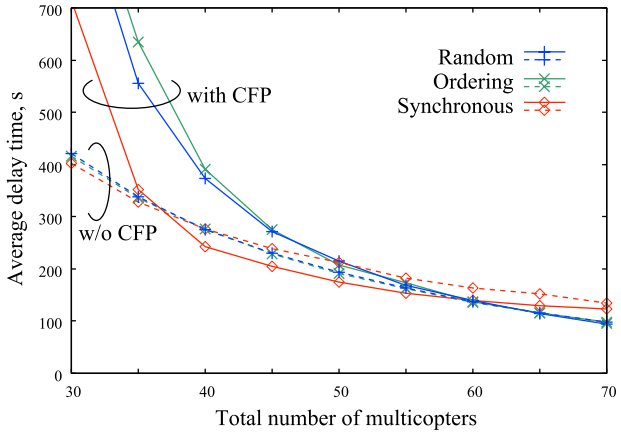

Fig. 8 Average delay time of the random, ordering, and synchronous drop timings for the rebounding flight scheme.

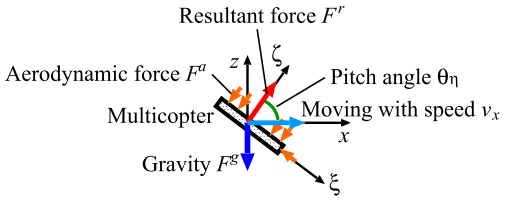

Fig. 9 Dynamic model of a flying multicopter.

5. Consideration of Multicopters' Inclination

A multcopter flies while inclining forward. This inclination affects the received power, and the communication range changes based on the inclination as well. In this section, we evaluate the delay time by formulating the received power and considering the multicopters' inclination.

5.1 Relationship between Moving Speed and Inclination

Here, we derive the relationship between the moving speed and the inclination of a multicopter. For simplification, a multicopter is represented by a cuboid, and Fig. 9 shows a dynamic model of a flying multicopter. A multicopter is moving in the x-axis direction with speed v_x. The axes ξ and ζ is defined as longitudinal and vertical directions of the multicopter, respectively. The pitch angle θ_η is an angle between the x-axis and the ζ-axis. In the dynamic model, the resultant force F^r by rolling propellers, the aerodynamic force F^a, and the gravitational force F^g are considered.

From the dynamic model, the motion equations in the x and y axes is derived by:

$$\begin{aligned} m\ddot{x} &= F^r \cos\theta_\eta - F^a_\zeta \cos\theta_\eta - F^a_\xi \sin\theta_\eta \\ &= (F^r - F^a_\zeta)\cos\theta_\eta - F^a_\xi \sin\theta_\eta, \end{aligned} \tag{1}$$

$$\begin{aligned} m\ddot{z} &= F^r \sin\theta_\eta - F^a_\zeta \sin\theta_\eta + F^a_\xi \cos\theta_\eta - F^g \\ &= (F - F^a_\zeta)\sin\theta_\xi + F^a_\xi \cos\theta_\eta - F^g, \end{aligned} \tag{2}$$

where F^a_i represents the i-axis component of the aerodynamic force. The gravitational force is derived by $F^g = mg$,

where m and g are the weight of the multicopter and the gravitational acceleration, respectively. We assume that the multicopter moves in the horizontal plane with a constant speed, whereas the acceleration in the x and z axes is 0. Then from (1) and (2), the following equation is obtained:

$$mg\cos\theta_\xi = F^a_\xi. \tag{3}$$

Let C_i, v_i, U_i, and A_i be the resistance coefficient, moving speed, wind speed, and swept area of the i axis, respectively, where $i \in \{\xi, \zeta\}$. The aerodynamic force is obtained by [13] as:

$$F^a_i = \frac{1}{2}\rho C_i (v_i - U_i)^2 A_i, \tag{4}$$

where ρ is air density. The wind speed is assumed to be 0. From (4) and $v_\xi = v_x \sin\theta_\eta$, the following equations is derived:

$$F^a_\xi = \frac{1}{2}\rho C_\xi (v_x \sin\theta_\eta)^2 A_\xi. \tag{5}$$

From (3) and (5), the pitch angle θ_η of the moving speed v_x is obtained by:

$$\theta_\eta = \cos^{-1}\left\{\sqrt{\left(\frac{mg}{\rho C_\xi A_\xi v_x^2}\right)^2 + 1} - \frac{mg}{\rho C_\xi A_\xi v_x^2}\right\}. \tag{6}$$

The angle θ_v between the multicopter's inclination and the horizontal plane is expressed as:

$$\theta_v = 90^\circ - \theta_\eta. \tag{7}$$

5.2 Calculation of Received Power Considering Inclination

The multicopter's inclination affects the received power because of the antenna directivity and the deviation of the polarization plane. When the transmitted power is P_t, the received power P_r can be modeled by:

$$P_r = P_t + G_t + G_r + G_p + G_d \text{ dBm}, \tag{8}$$

where G_t and G_r are the relative antenna gains of the directivity at a transmitter and a receiver, respectively, G_p is the gain of the polarization plane deviation, and G_d is the path loss gain.

5.2.1 Relative Antenna Gain

The multicopter deploys an omnidirectional antenna because it can connect the neighboring multicopters in the whole directions. The omnidirectional antenna does not have directivity in the horizontal plane, whereas it has directivity in the vertical plane. The antenna gain degrades when the multicopter inclines, which we call the relative antenna gain.

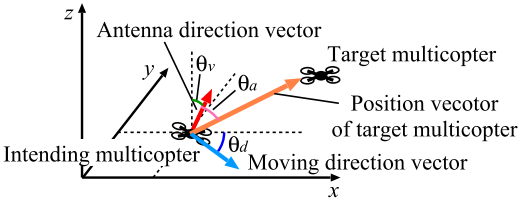

Fig. 10 A model of intending and target multicopters to calculate relative antenna gain.

Figure 10 shows a model of intending and target multicopters to derive the relative antenna gain. The target multicopter is a receiver if the intended multicopter is a transmitter, and vice versa. In this model, we use three vectors: the moving direction vector, the antenna direction vector $\boldsymbol{d}$, and the position vector $\boldsymbol{p}$ of the target multicopter. Let θ_d be the angle between the moving direction vector and the x-axis. The angle between the antenna direction vector and the position vector of the target multicopter is θ_a.

The antenna direction vector of the non-inclination of the multicopter is defined as $\boldsymbol{e} = (0\ 0\ 1)$. The antenna direction vector $\boldsymbol{d}$ can be calculated by rotating $\boldsymbol{e}$ in the x-axis direction with $-\theta_v$ around the y-axis and re-rotating it with $-\theta_d$ around the z-axis, i.e.,

$$\begin{aligned}\boldsymbol{d} = \boldsymbol{e}&\begin{pmatrix}\cos\theta_v & 0 & -\sin\theta_v\\ 0 & 1 & 0\\ \sin\theta_v & 0 & \cos\theta_v\end{pmatrix}\\ &\begin{pmatrix}\cos\theta_d & \sin\theta_d & 0\\ -\sin\theta_d & \cos\theta_d & 0\\ 0 & 0 & 1\end{pmatrix}\\ =&\begin{pmatrix}\sin\theta_v\cos\theta_d & \sin\theta_v\sin\theta_d & \cos\theta_v\end{pmatrix},\end{aligned} \tag{9}$$

where θ_d is positive when the intended multicopter moves to the positive direction in the y-axis and negative otherwise. Then, the angle θ_a is obtained by:

$$\theta_a = \cos^{-1}\frac{\boldsymbol{d}\cdot\boldsymbol{p}}{|\boldsymbol{d}||\boldsymbol{p}|}. \tag{10}$$

When the multicopter uses a dipole antenna, the relative antenna gain G_k in the vertical plane is expressed by [14] as:

$$G_k = 10\log_{10}\left\{\frac{\cos\left(\frac{\pi}{2}\cos\theta_a\right)}{\sin\theta_a}\right\}^2 \text{dB}, \tag{11}$$

where k represents a transmitter (t) or a receiver (r).

5.2.2 Gain of Polarization Plane Deviation

Since the antenna pattern in the horizontal plane is omnidirectional, the antenna is vertically attached to the multicopter. Therefore, the polarization plane is vertical. When the multicopter inclines, the polarization plane has a tilt, too. The deviation of the polarization planes between a transmitter and a receiver loses the gain defined by G_p.

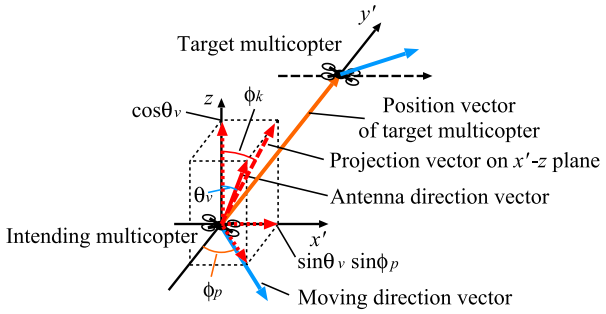

Fig. 11 A model of intending and target multicopters to calculate gain of polarization plane deviation.

Figure 11 shows a model of intending and target multicopters to calculate the gain of the polarization plane deviation. In the figure, new axes x' and y' are defined instead of the x and y axes. The y' axis represents the direction from the intending multicopter to the target one, and its origin is the location of the intending one. The x' axis is the direction orthogonal to the y' axis.

The angles of the position vector of the target multicopter and the moving direction vector are ϕ_p, and the angle of the z-axis and the projection vector of an antenna direction vector on the x'-z plane is ϕ_k, where k indicates a transmitter (t) or a receiver (r). When the magnitude of the antenna direction vector is 1, the x' and z components of the vector are $\sin\theta_v \sin\phi_p$ and $\cos\theta_v$, respectively. Therefore, the angle ϕ_k is derived by:

$$\phi_x = \tan^{-1} \frac{\sin\theta_v \sin\phi_p}{\cos\theta_v}. \tag{12}$$

The angle of the polarization plane deviation can be derived from the projection vectors on the $x' - z$ plane of transmitter's and receiver's antenna direction vector, which can be expressed as:

$$\phi = \begin{cases} |\phi_t - \phi_r| & \text{(both multicopters move} \\ & \text{in the same direction)} \\ |\phi_t + \phi_r| & \text{(otherwise)} \end{cases}. \tag{13}$$

The gain G_p of the polarization deviation is obtained by:

$$G_p = 10\log_{10}\cos^2\phi \text{ dB}. \tag{14}$$

5.2.3 Path Loss Gain

The multicopters fly in the sky, and the received signal is hardly affected by the ground reflection waves. Therefore, the path loss gain is assumed to obey the free space propagation model, in which the path loss gain G_d of the distance d is derived by [15] as:

$$G_d = 20\log_{10}\left(\frac{\lambda}{4\pi d}\right)\text{dB}, \tag{15}$$

where λ is the wavelength.

Table 4 Simulation settings for the evaluation considering multicopters' inclination.

Parameters of aerial wireless relay network	
Simulation area	4000 m × 4000 m
Position of source node	(500, 500)
Position of destination node	(3500, 3500)
Moving speed	10, 15, 20 m/s
Transmitted power	10 dBm
Threshold of received power for successful transmissions	−85 dBm
Aerodynamic force parameters	
Air density ρ	1.293 kg/m^3
Resistance coefficient C_ξ	0.40
Swept area A_ξ	0.03 m^2

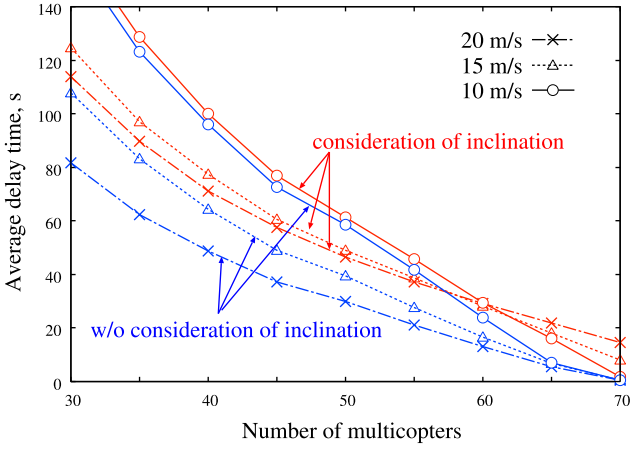

Fig. 12 Average delay time considering inclination of multicopters.

5.3 Delay Time Evaluation Considering Inclination

Table 4 shows the simulation settings. All multicopters move according to the rebounding flight scheme. The CFP is not deployed. The moving speed is 10, 15, and 20 m/s. The transmitted power is 10 dBm. The received power is calculated by (8), (11), (14), and (15). A packet is transmitted successfully if the the received power is more than a predefined threshold, −85 dBm. The aerodynamic force parameters are decided by [13] based on the specifications of DJI Phantom 4.

Figure 12 shows the average delay time considering the inclination of multicopters. We confirm that the consideration of multicopters' inclination causes an increase in the average delay time. When the inclination is not considered, fast movement of multicopters can reduce the average delay time. However, this relationship is not always valid for the case of considering the inclination. The delay time with moving speed 20 m/s takes the longest when the number of multicopters is more than 60. For the case of dense multicopters, frequent rebounding causes the stay of the multicopters in a small region. In this case, the average delay time increases because of the reduction of communication range due to the multicopters' inclination.

To evaluate the effect of moving speed on the average

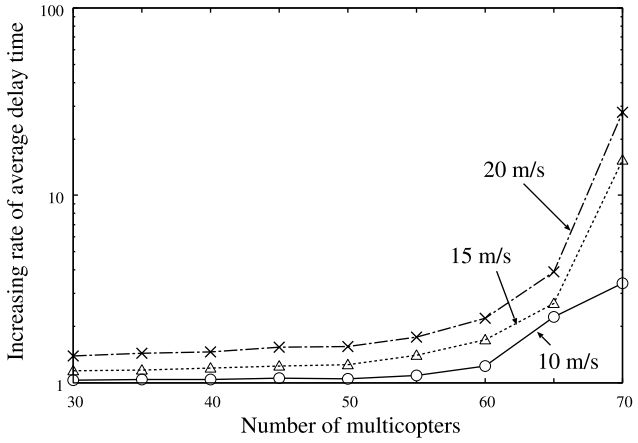

Fig. 13 Increasing rate of average delay time considering the inclination of multicopters.

delay time more clearly, Fig. 13 shows the increasing rate of average delay time by considering the multicopters' inclination. Thus, the faster the moving speed is, the larger the increasing rate of the average delay time is. In other words, the effect of the tilt is significant when the moving speed is fast. Furthermore, the increasing rate becomes more significant as the number of multicopters is large. Therefore, we reconfirm that the effect of rapid movement is unattainable for the case of dense multicopters.

6. Conclusions

We have reviewed the flight schemes in the AWRN using multicopters. From the simulation results, we found that the rebounding and CFP flight schemes are sufficient to reduce the average delay time. As the issues particularized for the AWRN, we have investigated the effects of drops due to battery capacity depletion and the inclination of moving multicopters. The rebounding flight scheme can compensate for the drops of the multicopters. From the result, there is an optimum moving as we consider the effects of the inclination.

The flight schemes discussed in this paper is based on simple operations. To reduce the delay time, especially for the small number of multicopters, we shall further improve the flight schemes in the future work while keeping autonomous movement [16].

Acknowledgments

The author would like to thank Mr. Jyo Suzuki, Mr. Hiroki Yanai, Prof. Kentaro Kobayashi, Prof. Takaya Yamazato, and Prof. Masaaki Katayama of Nagoya University. This work is supported in part by JSPS KAKENHI Grant Number 19K04392.

References

[1] H. Suzuki, Y. Kaneko, K. Mase, S. Yamazaki, and H. Makino, "An ad hoc network in the sky, SKYMESH, for large-scale disaster recovery," IEEE Vehicular Technology Conference, Sept. 2006. DOI:10.1109/VTCFall.2019.8891275.
[2] T. Umeki, H. Okada, and K. Mase, "Evaluation of wireless channel quality for an ad hoc network in the sky, SKYMESH," IEEE International Symposium on Wireless Communication Systems, pp.585–589, 2009.
[3] H. Okada, H. Oka, and K. Mase, "Network construction management for emergency communication system SKYMESH in large scale disaster," IEEE International Workshop on Management of Emerging Networks and Services, pp.875–880, 2012.
[4] Z.M. Fadlullah, D. Takaishi, H. Nishiyama, N. Kato, and R. Miura, "A dynamic trajectory control algorithm for improving the communication throughput and delay in UAV-aided networks," IEEE Netw., vol.30, no.1, pp.100–105, Jan. 2016.
[5] A. Mori, H. Okada, K. Kobayashi, M. Katayama, and K. Mase, "Construction of a node-combined wireless network for large-scale disasters," IEEE Consumer Communications and Networking Conference, pp.219–224, 2015.
[6] H. Yanai, H. Okada, K. Kobayashi, and M. Katayama, "Flight schemes considering breaks for wireless relay networks using drones during large-scale disasters," IEEE Vehicular Technology Conference, Aug. 2018. DOI:10.1109/VTCFall.2018.8690913.
[7] H. Yanai, H. Okada, K. Kobayashi, and M. Katayama, "Flight models in wireless relay networks using drones for large-scale disasters," IEICE Trans. Commun., vol.J103-B, no.2, pp.57–66, Feb. 2020 (in Japanese).
[8] M.J. Khabbaz, C.M. Assi, and W.F. Fawaz, "Disruption-tolerant networking: A comprehensive survey on recent developments and persisting challenges," IEEE Commun. Surveys Tuts., vol.14, no.2, pp.607–640, 2nd Quarter 2012.
[9] H. Okada, J. Suzuki, H. Yanai, K. Kobayashi, and M. Katayama, "Inclination of flying drones in aerial wireless relay networks," IEEE Vehicular Technology Conference, Sept. 2019. DOI:10.1109/VTCFall.2019.8891275.
[10] T. Camp, J. Boleng, and V. Davies, "A survey of mobility models for ad hoc network research," Wirel. Commun. Mob. Comput., vol.2, no.5, pp.483–502, Aug. 2002.
[11] C. Bettstetter, G. Resta, and P. Santi, "The node distribution of the random waypoint mobility model for wireless ad hoc networks," IEEE Trans. Mobile Comput., vol.2, no.3, pp.257–269, July–Sept. 2003.
[12] C. Bettstetter, "Mobility modeling in wireless networks: Categorization, smooth movement, and border effects," ACM Mobile Comput. Commun. Rev., vol.5, no.3, pp.55–66, July 2001.
[13] T. Nomura and T. Kobayashi, "A fundamental study on flight modelling of drone," Summaries to Technical Papers of Annual Meeting, Japan Association for Wind Engineering, pp.149–150, 2017.
[14] S. Silver, ed., Microwave Antenna Theory and Design, McGraw-Hill, 1949.
[15] J.G. Proakis and M. Salehi, Digital Communications, 5th ed., McGraw-Hill, 2007.
[16] H. Yanai, H. Okada, K. Kobayashi, and M. Katayama, "An emergency communication system using drones for large-scale disaster — An study on flight model using estimation of drones' positional distribution —," IEICE Technical Report, SeMI2019-138, March 2020 (in Japanese).

Hiraku Okada received the B.S., M.S. and Ph.D. degrees in Information Electronics Engineering from Nagoya University, Japan in 1995, 1997 and 1999, respectively. From 1997 to 2000, he was a Research Fellow of the Japan Society for the Promotion of Science. He was an Assistant Professor at Nagoya University from 2000 to 2006, an Associate Professor at Niigata University from 2006 to 2009, and an Associate Professor at Saitama University from 2009 to 2011. Since 2011, he has been an Associate Professor at Nagoya University. His current research interests include wireless communication systems, wireless networks, inter-vehicle communications, and visible light communication systems. He received the Inose Science Award in 1996, the IEICE Young Engineer Award in 1998, the IEICE Communications Society ComEX Best Letter Award in 2014, and the IEEE CCNC Best Paper Award in 2020. Dr. Okada is a member of IEEE and ACM.